First-principles study of the magnetic hyperfine field in Fe and Co multilayers

G. Y. Guo
Daresbury Laboratory, Warrington WA4 4AD, United Kingdom

H. Ebert
Institute for Physical Chemistry, University of München, Theresienstrasse 37, D-80333 München, Germany
(Received 8 August 1995)

We present *ab initio* calculations of the magnetic hyperfine field and magnetic moments in several Fe and Co multilayers ($(Fe(Co)_2Cu_6$ fcc (001), $FeCu(Ag)_5$ fcc (001), bcc Fe/fcc Ag_5 (001), bcc Fe_n/fcc Au_5 (001) ($n=1,3,7$), Co_kPd_1 fcc (111) [$k(l)=1$ (5), 2 (4), 3 (3)] and Co_2Pt_m fcc (111) ($m=1,4,7$)) as well as in bcc Fe and fcc (hcp, bcc) Co. The first-principles spin-polarized, relativistic linear muffin-tin orbital method is used. Therefore, both the orbital and magnetic dipole contributions as well as the conventional Fermi contact term are calculated. Calculations have been performed for both in-plane and perpendicular magnetizations. The calculated hyperfine field and its variation with crystalline structure and magnetization direction in both Fe and Co are in reasonable agreement (within 10%) with experiments. The hyperfine field of Fe (Co) in the interface monolayers in the magnetic multilayers is found to be substantially reduced compared with that in the corresponding bulk metal, in strong contrast to the highly enhanced magnetic moments in the same monolayers. It is argued that the magnetic dipole and orbital contributions to the hyperfine field are approximately proportional to the so-called magnetic dipole moment and the orbital moment, respectively. These linear relations are then demonstrated to hold rather well by using the calculated non-*s*-electron hyperfine fields, orbital and magnetic dipole moments. Unlike in the bulk metals and alloys, the magnetic dipole moment in the multilayers is predicted to be comparable to the orbital moment and as a result, the magnetic dipole contribution to the hyperfine field is large. The anisotropy in the hyperfine field is found to be very pronounced and to be strongly connected with the large anisotropy in the orbital moment and magnetic dipole moment. The induced magnetic moments and hyperfine fields in the nonmagnetic spacer layers are also calculated. The results for the multilayers are compared with available experiments and previous nonrelativistic calculations.

I. INTRODUCTION

The magnetic hyperfine field of an atom (or ion) in a solid is the magnetic field at the site of the atomic nucleus produced by the electrons in the solid. It describes the hyperfine interaction between the magnetic moment of the nucleus and the magnetic moment of the electrons in the solid. The hyperfine field may be measured by the nuclear methods such as the Mössbauer effect and the nuclear magnetic resonance (NMR). For example, the hyperfine field in the Fe atoms can be determined by the isotope ^{57}Fe Mössbauer effects,[1] while the hyperfine field of Co and Cu may be determined by, respectively, the ^{59}Co (Ref. 2) and $^{63(65)}$Cu (Ref. 3) nuclear magnetic resonances. The hyperfine field in the Au atoms can be measured by both the isotope ^{197}Au Mössbauer effect[4] and ^{197}Au NMR.[5] Apart from fundamental interest in their own right, the magnetic hyperfine fields in a solid provide valuable information about the electronic structure and magnetic properties of the solid.[1] In the first place, the hyperfine field of a magnetic atom may be related to the local magnetic moment on the atom. For instance, the variation of the average hyperfine field with alloy composition for several series of iron alloys was found to be similar to that of the averaged magnetic moment in the same alloys.[6] Second, the hyperfine field technique is element and site selective. It has been widely used to probe the local environment and the coordination number of the atoms studied.[7,8] Third, the hyperfine field is also a valuable probe of the electronic spin density distributions near the nuclei in a magnetic solid.

One of the important applications of the magnetic hyperfine technique at present is the study of magnetism in magnetic multilayers and thin films.[1,3,4,7–9] Indeed, the hyperfine field method has been used to determine the magnetic anisotropy of, e.g., ultrathin Fe(100) films on Ag(100),[10] the Fe/Co and Fe/Cu multilayers,[11] and also to study induced magnetization of nonmagnetic metallic spacers in, e.g., the Fe/Cu (Ref. 3) and Fe/Au (Ref. 4) multilayers. Furthermore, recent monolayer-probe ^{57}Fe Mössbauer experiments[12,13] has been used to study the surface and interface induced Friedel oscillations of magnetization or hyperfine field in the Fe/W bilayers predicted earlier.[14]

In this paper, we report the calculated hyperfine fields and magnetic moments in Fe and Co as well as their multilayers. The present calculations were based on the first-principles relativistic, spin-polarized density functional theory.[15] Both core and band states were treated fully relativistically by solving the effective one-electron spin-polarized Dirac equation.[16,17] Furthermore, a fully relativistic hyperfine interaction operator was used. By the Breit reduction or the Foldy-Wouthuysen transformation, one can relate the relativistic theory to a perturbation expansion starting with the nonrelativistic limit[18–20] (see also Sec. II). In the lowest order, the relativistic hyperfine interaction operator reduces to three terms, namely, the Fermi-contact, magnetic dipole, and orbital terms. For cubic systems, the last two terms are purely relativistic corrections but the first term also exists in the

nonrelativistic theory. One of the main objectives of this paper is to understand the relative importance of various contributions to the hyperfine interaction in the magnetic multilayers. There are several reports on the theoretical hyperfine fields in the Fe, Co, and Ni surfaces and overlayers in the literature mainly by Freeman and co-workers.[14,21–23] However, in these previous calculations, only the Fermi contact term was calculated because the band electrons were treated scalar relativistically.[24] Fully relativistic calculations of the magnetic hyperfine fields have been performed for transition metals and their alloys,[16,25,26] although they have not been carried out for magnetic multilayers. These calculations demonstrated that due to spin-orbit coupling, the orbital contribution is rather significant in these bulk systems.[16,25,26] Because of much reduced symmetry near the surface and the interface, which generally enhances both spin and orbital moments (see, e.g., Refs. 14, 21–23, and 27), the orbital contribution to the hyperfine field is expected to be even more important. So far, little attention has been paid to the magnetic dipole contribution although it may be expected to be negligibly small in the bulk systems. In this paper we argue that the magnetic dipole contribution is comparable to the orbital contribution in the multilayer systems.

Another main objective of this paper is to study the anisotropy in the hyperfine interaction in the multilayer systems. This could not be done in the previous calculations[14,21–23] because only scalar-relativistic calculations were performed. We recently found that even in hcp Co, the anisotropy in the hyperfine field is already significant.[28] It is also important to understand the anisotropy in the hyperfine field and its connections to the other magnetic anisotropies in magnetic multilayers, since the hyperfine field technique is increasingly being used to probe the magnetic anisotropies in the multilayer systems. Finally, one other main objective of this paper is to reveal simple relationships between various (spin, orbital, and magnetic dipole) moments and various (Fermi-contact, orbital, and magnetic dipole) hyperfine fields. It is found that except the valence electron Fermi contact term, which is related in a complicated manner to the electronic structure of the system under investigation, the variation of the core, orbital, and magnetic dipole hyperfine fields, respectively, follows that of the spin, orbital, and magnetic dipole moments.

The organization of this paper is as follows. In Sec. II we summarize the relativistic theory of the hyperfine field and its relations to the nonrelativistic perturbation approach. Also in Sec. II, we describe the computational method and details. In Sec. III, we compare the calculated hyperfine fields in the bulk Fe and Co with experiments as well as previous calculations. Having found that the present fully relativistic approach gives rather reliable hyperfine fields for the bulk Fe and Co, we then report the results for the Fe and Co multilayers in Sec. IV. In Sec. IV we also study the features and trends of the calculated hyperfine fields. In Sec. V we discuss possible correlations between the magnetic moments and various components of the hyperfine field. We also compare the calculated hyperfine fields in the multilayer systems with previous calculations and experiments. Finally, a summary is given in Sec. VI.

II. THEORY AND COMPUTATIONAL METHOD

For an atomic nucleus possessing a magnetic moment, there is a magnetic hyperfine interaction between the nucleus and an electron, in addition to the usual Coulombic interaction between them. In the fully relativistic approach, this hyperfine interaction operator is[29]

$$H_{\rm hf}=e\alpha\cdot\mathbf{A_n}=e\alpha\cdot(\mu_{\mathbf{n}}\times\mathbf{r})/r^3, \tag{1}$$

where e is the electronic charge, α are the Dirac 4×4 matrices, $\mathbf{A}_n$ is the vector potential due to the magnetic moment μ_n of the nucleus, and $\mathbf{r}$ is the distance vector between the nucleus and the electron. To the observer stationed on the nucleus, the hyperfine interaction is caused by the magnetic field (hyperfine field $B_{\rm hf}$) produced by the electronic spin and orbital currents in the vicinity of the nucleus. In the relativistic band theory, the hyperfine field due to the valence (or band) electrons is given by[16,30]

$$B^v_{\rm hf}=\mu_n^{-1}\sum_{j,\mathbf{k}}\langle\Psi_{j\mathbf{k}}|e\alpha\cdot\mathbf{A_n}|\Psi_{j\mathbf{k}}\rangle w_{j\mathbf{k}}\theta(E_F-E_{j\mathbf{k}}), \tag{2}$$

where E_F is the Fermi energy and $\Psi_{j\mathbf{k}}$ ($E_{j\mathbf{k}}$) the band-state wave function (energy). The weight for wave vector $\mathbf{k}$ and band j, $w_{j\mathbf{k}}$, determined by the energy bands, is evaluated by using the tetrahedron method.[31,30] Similarly, in the fully relativistic approach, the hyperfine field due to the core electrons is given by[17]

$$B^c_{\rm hf}=\mu_n^{-1}\sum_{n\kappa\mu}\langle\Phi_{n\kappa\mu}|e\alpha\cdot\mathbf{A_n}|\Phi_{n\kappa\mu}\rangle, \tag{3}$$

where $\Phi_{n\kappa\mu}$ is the core-state wave function. In this work, both the core and valence wave functions are four component bispinors[29] and, in the framework of the relativistic, spin-polarized density-functional theory,[15] are the self-consistent solutions to the effective one-electron Dirac Hamiltonian

$$H_D=\frac{c}{i}\,\alpha\cdot\nabla+\frac{c^2}{2}(\beta-I)+V(\mathbf{r})+\beta\sigma\cdot\mathbf{B}(\mathbf{r}), \tag{4}$$

where $V(\mathbf{r})$ is the spin-averaged part of the effective one-electron potential and $\beta\sigma\cdot\mathbf{B}(\mathbf{r})$ is the spin-dependent part of the potential.

It is useful to relate purely relativistic theory of the hyperfine interaction to the perturbation approach for treating relativistic effects starting from the nonrelativistic limit. This will allow us to make comments on previous nonrelativistic or scalar-relativistic calculations. Furthermore, it will make the relativistic corrections more transparent. The relativistic expressions for the hyperfine field in a perturbation approach has been derived before by several groups.[18–20] In the lowest order, $H_{\rm hf}$ reduces in the nonrelativistic limit to the form[19]

$$H_{\rm hf}\approx\frac{8\pi}{3}\,\mu_B\mu_n\cdot\sigma\delta(\mathbf{r})-\mu_B[\mu_n\cdot\sigma/r^3-3(\mu_n\cdot\mathbf{r})(\sigma\cdot\mathbf{r})/r^5]+2\mu_B(\mu_{\mathbf{n}}\cdot\mathbf{L})/r^3, \tag{5}$$

which consists of conventional Fermi-contact, nuclear moment-electron magnetic dipole and nuclear moment-

electron orbital interaction terms. Accordingly, the hyperfine field $B_{\rm hf}$ can be decomposed into three terms given by

$$B_{\rm hf} \approx B^s_{\rm hf} + B^d_{\rm hf} + B^0_{\rm hf} = B^s_{\rm hf} + B^{\rm ns}_{\rm hf} \tag{6}$$

where $B^s_{\rm hf}$ is the Fermi-contact term due to the s electrons and $B^{\rm ns}_{\rm hf}$ the magnetic dipole and orbital terms due to the non-s electrons. Note that Eq. (5) should be used only in the nonrelativistic electronic structure calculations and in the scalar-relativistic calculations, a similar expression derived by Blügel *et al.*[20] should be used. The non-s electron contribution has often been called the orbital hyperfine field because the orbital part is usually assumed to be dominant (see Refs. 25 and 26 and references therein). Indeed, this appears to be the case for bulk metals and alloys.[25,26] However, it is found in this work that due to the reduced symmetry in the magnetic multilayers, the magnetic dipole contribution may be comparable to the orbital contribution. This appears to be consistent with recent calculations,[32,33] which showed that although the so-called magnetic dipole moment is generally negligible in the bulks, it is comparable to that of the orbital magnetic moment in the magnetic multilayers, overlayers and thin films. Importantly, it is also found that in the same way as the orbital field is related to the orbital moment, the magnetic dipole field can be related to the magnetic dipole moment, which enters the recently derived spin sum rule for the circular magnetic x-ray dichroism.[34] To make connections between the magnetic dipole and orbital components of the non-s-electron hyperfine field ($B^{\rm ns}_{\rm hf}$) and the magnetic dipole and orbital moments, one can make the following approximations

$$B^d_{\rm hf} = -\mu_B \sum_{j\mathbf{k}} \left\langle \psi_{j\mathbf{k}} \middle| \left[1 - 3\frac{z^2}{r^2}\right] \frac{\sigma_z}{r^3} \middle| \psi_{j\mathbf{k}} \right\rangle w_{j\mathbf{k}} \approx -\langle r^{-3}\rangle \left\{ \mu_B \sum_{j\mathbf{k}} \left\langle \psi_{j\mathbf{k}} \middle| \left[1 - 3\frac{z^2}{r^2}\right] \sigma_z \middle| \psi_{j\mathbf{k}} \right\rangle w_{j\mathbf{k}} \right\} = -\langle r^{-3}\rangle m_d , \tag{7a}$$

$$B^0_{\rm hf} = \mu_B \sum_{j\mathbf{k}} \left\langle \psi_{j\mathbf{k}} \middle| 2\frac{l_z}{r^3} \middle| \psi_{j\mathbf{k}} \right\rangle w_{j\mathbf{k}} \approx 2\langle r^{-3}\rangle \left\{ \mu_B \sum_{j\mathbf{k}} \langle \psi_{j\mathbf{k}} | l_z | \psi_{j\mathbf{k}} \rangle w_{j\mathbf{k}} \right\} = 2\langle r^{-3}\rangle m_0 , \tag{7b}$$

$$\frac{B^d_{\rm hf}}{B^0_{\rm hf}} \approx \frac{-m_d}{2m_0} = -R,$$

$$B^0_{\rm hf} \approx \frac{B^{\rm ns}_{\rm hf}}{(1-R)}, \tag{7c}$$

$$B^d_{\rm hf} \approx -\frac{RB^{\rm ns}_{\rm hf}}{(1-R)},$$

where m_d is the magnetic dipole moment and m_0 the orbital moment. $\langle r^{-3}\rangle$ is the averaged expection value of r^{-3} of the radial wave functions. Equations (7c) will be used in Secs. IV and V to estimate the orbital and dipole hyperfine fields from the calculated non-s hyperfine field and magnetic dipole and orbital moments. Equation (7b), first suggested by Abragam and Pryce,[35] has often been used to estimate the non-s (or orbital) hyperfine field from the known orbital moment or vice versa.[5,36]

In this paper, we study the $Fe(Co)_2Cu_6$ fcc (001), $FeCu(Ag)_5$ fcc (001), bcc-Fe/fcc-Ag_5 (001), bcc-Fe_n/fcc-Au_5 (001) (n=1,3,7), Co_kPd_1 fcc (111) [$k(l)$=1 (5), 2 (4), 3 (3)] and Co_2Pt_m fcc (111) (m=1,4,7) multilayers. We also study bcc Fe, fcc, hcp, and bcc Co in order to evaluate the accuracy of the present fully relativistic approach, since the experimental hyperfine field data for these bulk systems are well documented. We first performed all-electron self-consistent electronic structure calculations using the spin-polarized, relativistic linear muffin-tin orbital (SPRLMTO) method.[16] These *ab initio* electronic structure calculations were based on the relativistic spin-density-functional theory[15] with Vosko-Wilk-Nusair (VWN) parametrization of the local density exchange-correlation potential.[37] Except for bcc-Fe_7/fcc-Au_5 (001), and Co_kPd_1 fcc (111) [$k(l)$=1 (5), 3 (3)], self-consistent electronic structure calculations have been reported before.[38] The way we choose the structural parameters, and the lattice constants and atomic radii used for these systems, have been given in Ref. 38. Therefore, it suffices to mention that the c/a ratio used is 7.036 for bcc-Fe_7/fcc-Au_5 (001), 4.809 for Co_1Pd_5 fcc (111) and 4.629 for Co_3Pd_3 fcc (111). The experimental lattice constant (2.825 Å) (Ref. 36) is used for bcc Co. In the previous paper,[38] however, von Barth–Hedin (vBH) parametrization of the local exchange-correlation potential[39] was used. The VWN parametrization is perhaps the most accurate one, especially in the extremely high- and low-density regions, and thus is used in this paper. Nevertheless, the differences in most calculated magnetic properties such as magnetic moments using both parametrizations are found to be negligibly small, although the difference in the core contribution to the hyperfine field can be as large as 10% (see Sec. III). In the self-consistent calculations, the basis functions used were s, p, and d MTO's, and the magnetization was assumed to be perpendicular to the Fe or Co monolayer planes (i.e., $\mathbf{m}\|[001]$). We used the analytic tetrahedron technique to perform the Brillouin-zone (BZ) integrations.[30] For the valence hyperfine-field calculations, larger basis sets and denser k meshes in the irreducible wedge (IW) of the BZ are neces-

TABLE I. Theoretical shell-decomposed hyperfine fields (in kG) of bcc Fe and fcc Co calculated self-consistently by the SPRLMTO method for $\mathbf{M}\|[001]$.

Shell	bcc Fe	fcc Co
$1s$	−20.5	−18.4
$2s$	−521.8	−436.9
$2p$	1.7	1.6
$3s$	291.0	260.9
$3p$	−0.7	0.7
Core sum	−250.2	−193.6
s	−72.8	−75.4
p	0.9	1.7
d	14.6	44.6
f	−0.3	−0.1
Valence sum	−57.7	29.2
Total	−307.9	−222.8
Experiment	−339[a]	−216[b]

[a]Reference 40.
[b]Reference 41.

sary. Therefore, the final band structures were generated with a larger basis of s, p, and d as well as f MTO's. Furthermore, the calculations were performed for both in-plane and perpendicular magnetizations in order to study the anisotropy in the hyperfine field. The number of k points over the IW used is 2457 (over 3/48 of the BZ) for bcc Fe (Co), 1515 (over 3/48 of the BZ) for fcc Co, 2187 (over 3/24 of the BZ) for hcp Co, 867 (over 2/16 of the BZ) for $Fe(Co)_2Cu_6$ fcc (001), bcc Fe_7/fcc Au_5 (001), 1156 (over 2/16 of the BZ) for $FeCu(Ag)_5$ fcc (001), bcc Fe/fcc Ag_5 (001), bcc Fe_n/fcc Au_5 (001) (n=1,3), 1194 (over 6/24 of the BZ) for $Co_2Pd(Pd)_4$ fcc (111), 3402 (over 6/24 of the BZ) for Co_2Pt_1 fcc (111), 1458 (over 6/24 of the BZ) for Co_2Pt_7 fcc (111). The results presented in this paper were found to be converged within a few percent with respect to the number of k points used.

III. RESULTS FOR BULK Fe AND Co

In this section, we present results for the bulk Fe and Co, and compare them with previous calculations as well as experiments. The shell-decomposed hyperfine fields for bcc Fe and fcc Co are listed in Table I, together with measurements.[40,41] As found before,[17] the contribution of non-s-core electrons is negligible (Table I). This can be expected from Eqs. (7a) and (7b) because of the zero-core magnetic dipole and orbital moments. Note that because of spin-orbit coupling, local magnetic dipole and orbital magnetization densities can be slightly nonzero, e.g., near the nuclei, which gives rise to a tiny non-s-core hyperfine field. In contrast, the contribution of non-s-valence electrons ($B_{\rm hf}^{\rm ns}$), in particular, d electrons, is comparable to the s valence electron contribution (Table I). Furthermore, the non-s-valence electron hyperfine field ($B_{\rm hf}^{\rm ns}$) has a positive sign, opposite to that of the s-valence electron hyperfine field. Table I indicates that the calculated hyperfine field in both bcc Fe and fcc Co is in good agreement with experiment, and the discrepancy between theory and experiment is within 10%. Hereafter, we simply refer to the contribution of all the core electrons, of the s-valence electrons and of the non-s-valence electrons, respectively, as the core hyperfine field ($B_{\rm hf}^{c}$), s-electron hyperfine field ($B_{\rm hf}^{s}$) and non-s-electron hyperfine field ($B_{\rm hf}^{\rm ns}$).

For comparison, the results of some previous calculations[42,43,16] are listed in Table II. It is clear from Table II that the hyperfine field in bcc Fe (−260 kG) obtained by nonrelativistic self-consistent Korringa-Kohn-Rostoker (KKR) calculations[42] is much smaller than the experimental value (−339 kG).[40] Nevertheless, the result of the same nonrelativistic calculations for fcc Co is in reasonable agreement with experiment (Tables I and II). Self-consistent, scalar-relativistic calculations for bcc Fe (Ref. 43) were in very good agreement with experiment (see Tables I and II). Interestingly, relativistic calculations[16] showed that including relativistic corrections for bcc Fe increased the discrepancy between theory and experiment (more than 20%), suggesting that the good agreement between previous scalar-relativistic calculations[43] and experiments was fortuitous. Indeed, as shown by Blügel *et al.*,[20] simply inserting the scalar-relativistic wave functions into the nonrelativistic Fermi contact hyperfine matrix expression [Eq. (5)] is incorrect and can lead to a significant overestimation of the relativistic corrections.

As mentioned earlier, a good agreement is found between

TABLE II. Comparison of theoretical hyperfine fields (in kG) obtained in this work with previous calculations. SC denotes self-consistent calculations. vBH means von Barth–Hedin local density potential (Ref. 39) being used. VWN means Vosko-Wilk-Nusair local potential (Ref. 37) being used.

Method	Basis	bcc Fe $B_{\rm hf}$ ($B_{\rm hf}^{v}$,$B_{\rm hf}^{c}$)	fcc Co $B_{\rm hf}$ ($B_{\rm hf}^{v}$,$B_{\rm hf}^{c}$)
SC-SPRLMTO (vBH)	s,p,d,f	−288.2 (−50.7, −237.5)	−206.9 (−28.1, −179.0)
SC-SPRLMTO (VWN)	s,p,d	−301.5 (−51.3, −250.2)	−208.4 (−17.5, −193.6)
	s,p,d,f	−307.9 (−57.7, −250.2)	−222.8 (−29.2, −193.6)
SPRLMTO[a]	s,p,d	−281.8 (−35.3, −231.5)	−201.1 (−28.0, −173.1)
SC-SRLMTO[b]	s,p,d	−338 (−71, −267)	
SC-KRR[c]	s,p,d,f	−260	−220

[a]Reference 16.
[b]Reference 43.
[c]Reference 42.

TABLE III. Calculated magnetic moments (in μ_B) and hyperfine fields (in kG) of Co in fcc, hcp, and bcc structures. m_s (m_o), $B_{\rm hf}$ ($B^c_{\rm hf}$), and $B^s_{\rm hf}$ ($B^{\rm ns}_{\rm hf}$) are, respectively, the spin (orbital) moment, total (core) and valence s-electron (non-s-electron) hyperfine fields. m_d is the magnetic dipole moment.

	m_s	m_o	m_d	$B^c_{\rm hf}$	$B^s_{\rm hf}$	$B^{\rm ns}_{\rm hf}$	$B^v_{\rm hf}$	$B_{\rm hf}$	$B^{\rm expt}_{\rm hf}$
fcc	1.631	0.074	0.0	−193.6	−75.4	46.2	−29.2	−222.8	−216[a]
hcp	1.596	0.077	−0.006	−190.5	−85.2	50.5	−34.5	−225.2	−219[b]
hcp[c]	1.596	0.072	0.004	−190.5	−85.2	44.5	−40.6	−231.1	−227[b]
bcc	1.743	0.080	0.0	−202.8	−20.9	50.3	29.4	−173.3	−166[a]

[a]Reference 41.
[b]Reference 36.
[c]Magnetization in the hexagonal planes of the hcp structure.

present calculations and experiment (see Table I). To reveal this apparent discrepancy between the present work and the previous relativistic calculations,[16] the hyperfine fields calculated by using different parametrizations of the local density exchange correlation potential and different basis sets are also listed in Table II. Part (about half for bcc Fe and most for fcc Co) of this discrepancy comes from the difference in the core contribution. This difference in the core hyperfine field ($B^c_{\rm hf}$) is mainly caused by the use of the different parametrizations of the local density exchange-correlation potential in this work and previous calculations,[16] and, to a lesser extent, is caused by the fact that in these previous calculations nonrelativistic self-consistent potentials generated for smaller lattice constants (2.73 Å for bcc Fe and 3.41 Å for fcc Co) in Ref. 42 were used. In the present calculations, the experimental lattice constants (2.86 Å for bcc Fe and 3.54 Å for fcc Co) were used. The difference in the valence contribution is large for bcc Fe. The significant factors responsible for this discrepancy in the valence contribution are the VWN local density potential and the larger basis set ($spdf$) used as well as the self-consistency carried out in this work. In short, to obtain accurate hyperfine fields, it is important to use the accurate parametrization of the local density exchange-correlation potential and a sufficiently large basis set, and to perform all-electron self-consistent calculations.

Co exists in nature in two crystalline structures, namely, hcp and fcc. Recently, a metastable bcc structure was stabilized by growing a film on a GaAs structure.[44] Therefore, Co is a particularly interesting element to study, since we can compare results on three different phases. We have calculated the hyperfine fields for both bcc Co and hcp Co, as well as fcc Co. These results are listed in Table III, together with experiments.[41,36] In agreement with experiment[41,36] we find that the bcc phase has a smallest hyperfine field (Table III). In agreement with previous calculations[45] but in disagreement with experiment,[44] we find that the bcc phase has the largest magnetic moment (Table III). The discrepancy of the Co magnetic moment between theory and experiment was previously attributed to the defects in the bcc films.[45] The magnetic moments and hyperfine fields in fcc and hcp Co were calculated before[28] in exactly the same way as in this work except that the vBH exchange-correlation potential[39] was used and the frozen core approximation was made. All the results except the core hyperfine field, of the present and previous calculations[28] agree well (within 2%).

Table III shows that the values of the calculated hyperfine field in all the Co structures agree well with the experimental values (within a few percent). Furthermore, it is clear from Table III that the observed variation in the hyperfine field with the change in either the crystalline structure or the magnetization direction is well reproduced by the present calculations. This gives us confidence to go on calculating the hyperfine fields in more complex Fe and Co magnetic multilayers with the present fully relativistic approach.

IV. MAGNETIC MOMENTS AND HYPERFINE FIELDS IN MULTILAYERS

A. Fe multilayers

Calculated Fe magnetic moments and hyperfine fields in the Fe multilayers are presented in Table IV. The orbital hyperfine field ($B^o_{\rm hf}$) is derived from the calculated non-s-electron hyperfine field ($B^{\rm ns}_{\rm hf}$), orbital moment (m_o) and magnetic dipole moment (m_d) by using Eqs. (7c). We note that while the magnetic moments on the Fe atoms in the interface monolayers are enhanced compared with those in the bulk bcc Fe, the hyperfine field ($B_{\rm hf}$) of Fe in the same monolayers, in contrast, is substantially reduced. This interface reduction is especially large (by up to 190 kG) in Fe_1Ag_5 fcc (001) and bcc-Fe_1/fcc-Ag_5 (001). Table IV shows that this comes about because the s-electron hyperfield ($B^s_{\rm hf}$) in the interface monolayers not only changes sign but also increases its magnitude. This change in the $B^s_{\rm hf}$ significantly overcompensates the increased magnitude in the core hyperfine field due to the interface enhanced spin moment (m_s). This reduction is further helped by the increase in the non-s-electron hyperfine field ($B^{\rm ns}_{\rm hf}$) in many systems due to the enhanced orbital moment (m_o) and magnetic dipole moment (m_d) (see Table IV).

Comparing the results for Fe_1Ag_5 fcc (001) and bcc-Fe_1/fcc-Ag_5 (001), one can study the effects of reducing the interface spacing between the Fe monolayer and neighboring Ag layers. One sees from Table IV that, because of the increased interface spacing, both the spin and orbital moments of Fe are larger in Fe_1Ag_5 fcc (001) than bcc-Fe_1/fcc-Ag_5 (001). Nevertheless, the total hyperfine field of Fe is also larger in Fe_1Ag_5 fcc (001) than bcc-Fe_1/fcc-Ag_5 (001). Although the positive non-s-electron hyperfine field is larger in Fe_1Ag_5 fcc (001) because of its larger orbital moment, its increase is overcompensated by the larger magnitude of the negative core hyperfine field (see Table IV). Interestingly, the s-electron hyperfine field is hardly affected

TABLE IV. Calculated magnetic moments (μ_B/atom) and hyperfine fields (kG) of Fe in bcc Fe and Fe multilayers. m_s (m_o), $B_{\rm hf}$ ($B^c_{\rm hf}$), and $B^s_{\rm hf}$ ($B^{\rm ns}_{\rm hf}$) are, respectively, the spin (orbital) moment, total (core), and s-electron (non-s-electron) hyperfine fields. m_d and $B^o_{\rm hf}$ are, respectively, the magnetic dipole moment and the orbital hyperfine field. Fen denotes Fe in the nth layer below the interface Fe layer.

System	Atom	m_s	m_o	m_d	$B_{\rm hf}$	$B^c_{\rm hf}$	$B^s_{\rm hf}$	$B^{\rm ns}_{\rm hf}$	$B^o_{\rm hf}$
bcc Fe		2.175	0.042		−307.9	−250.2	−72.8	15.2	15.2
Fe_2Cu_6	Fe	2.468	0.074	−0.030	−257.6	−278.2	−18.7	39.3	32.6
Fe_2Cu_6[a]		2.468	0.065	0.015	−272.5	−278.2	−18.8	24.4	27.5
Fe_1Cu_5	Fe	2.474	0.065	−0.087	−165.0	−275.9	67.1	43.8	26.3
Fe_1Cu_5[a]		2.474	0.056	0.043	−195.1	−275.9	67.1	13.6	22.1
Fe_1Ag_5	Fe	3.043	0.112	−0.150	−138.0	−336.4	114.2	84.2	50.5
Fe_1Ag_5[a]		3.043	0.086	0.074	−200.9	−336.4	114.2	21.3	38.2
bcc-Fe_1/Ag_5	Fe	2.832	0.094	−0.087	−121.0	−300.5	117.3	62.1	43.3
bcc-Fe_1/Ag_5[a]		2.830	0.071	0.043	−165.3	−300.5	117.2	18.0	26.0
bcc Fe_1/Au_5	Fe	2.850	0.035	−0.090	−170.4	−316.1	116.0	29.8	13.0
bcc Fe_1/Au_5[a]		2.847	0.005	0.045	−224.3	−316.1	115.0	−23.7	6.8
bcc Fe_3/Au_5	Fe	2.705	0.051	−0.007	−260.9	−304.3	24.1	19.3	20.6
	Fe1	2.322	0.046	−0.034	−352.3	−263.8	−111.7	23.2	16.9
bcc Fe_3/Au_5[a]	Fe	2.705	0.027	0.003	−278.6	−304.3	24.0	1.8	1.9
	Fe1	2.322	0.038	0.017	−367.5	−263.8	−112.0	8.3	10.7
bcc Fe_7/Au_5	Fe	2.707	0.063	−0.004	−204.2	−305.2	14.9	26.2	25.5
	Fe1	2.334	0.048	−0.014	−389.0	−267.0	−94.8	22.2	19.3
	Fe2	2.356	0.042	−0.0	−350.6	−271.0	−69.0	15.5	15.5
	Fe3	2.314	0.049	−0.004	−312.6	−268.5	−72.0	20.3	19.6
bcc Fe_7/Au_5[a]	Fe	2.707	0.029	0.001	−286.9	−305.2	14.9	3.3	3.4
	Fe1	2.334	0.044	0.007	−348.2	−267.0	−94.8	13.6	14.7
	Fe2	2.357	0.045	−0.0	−323.8	−271.0	−69.0	16.1	16.1
	Fe3	2.315	0.047	0.001	−323.4	−268.5	−72.0	17.1	17.3

[a]In-plane magnetization.

by the increased interface spacing (Table IV). The differences in the magnetic moments and hyperfine fields between Fe_1Cu_5 fcc (001) and Fe_1Ag_5 fcc (001) are mainly caused by the different lattice constants, namely, $a=2.557$ Å for Fe_1Cu_5 fcc (001) and $a=2.889$ Å for Fe_1Ag_5 fcc (001). bcc-Fe_1/fcc-Ag_5 (001) has a similar lattice constant (2.889 Å) to that of bcc-Fe_1/fcc-Au_5 (001) (2.884 A). Therefore, the differences in their magnetic properties are mainly caused by the different nonmagnetic substrate atoms. Surprisingly, the orbital moment and non-s hyperfine field of Fe in bcc-Fe_1/fcc-Au_5 (001) are significantly smaller than that in Fe_1Ag_5 fcc (001), although the spin moment, core, and s-electron hyperfine fields are, as expected, very similar in both systems (Table IV).

Table IV shows that there is a pronounced anisotropy in the hyperfine field in all the Fe magnetic multilayers studied. Furthermore, this anisotropy is almost completely caused by the anisotropy in the non-s-electron hyperfine field, which in term is correlated with the anisotropy in the magnetic dipole and orbital moments. In other words, there is no anisotropy in the core and s-electron hyperfine field. Therefore, fully relativistic calculations are essential to study the anisotropy in the hyperfine field. The percentage of the hyperfine anisotropy is rather striking. For example, the hyperfine anisotropy in bcc-Fe_1/fcc-Ag_5 (001) is well above 20%. Importantly, this, in conjunction with the site selectivity, suggests that hyperfine-field measurements are a very useful probe of the magnetic anisotropy in the magnetic multilayers and thin films.

The hyperfine fields of the nonmagnetic Cu and Au atoms in the Cu and Au magnetic multilayers have also been measured.[3,4] These experiments are useful to understand induced magnetization in the nonmagnetic spacer layer, which is generally believed to be important for the occurrence of the giant magnetoresistance and oscillatory exchange coupling in the magnetic multilayers. We therefore list the calculated Cu (Au) hyperfine fields in the Fe/Cu(Au) multilayers in Table V. It is clear that the Au hyperfine field in the interface Au monolayers is large, and it comes predominantly from the s-electron hyperfine field. Unlike Fe, both Cu and Au have a small core contribution (a few percent). The magnetic moments of Cu(Au) in the interface Cu(Au) monolayers are significant, while the magnetic moments of Cu(Au) in the central Cu(Au) [Cu(Au)2 in Table V] monolayers are negligible. Interestingly, the hyperfine-field anisotropy in the interface Au monolayers is notable (quite a few percent). This, again, is mainly because of the non-s-electron hyperfine field anisotropy. Nevertheless, there is no hyperfine field anisotropy in the first and second Au subinterface monolayers and in the Cu monolayers. It is also interesting to note that the magnetic moments and hyperfine fields of Au depend on the number of Fe monolayers in the Fe slabs in the Fe/Au multilayers. For example, the Au hyperfine field is reduced by nearly 20% when one moves from bcc-Fe_1/fcc-Au_5 (001) to bcc Fe_3/fcc Au_5 (001). Finally, in the bcc-$Fe_{3(7)}$/fcc-Au_5 (001) multilayers, the sign of the Au hyperfine field is oscillatory.

TABLE V. Calculated magnetic moments (μ_B/atom) and hyperfine fields (kG) of Cu(Au) in Fe/Cu(Au) multilayers. m_s (m_o), $B_{\rm hf}$ ($B^c_{\rm hf}$), and $B^s_{\rm hf}$ ($B^{\rm ns}_{\rm hf}$) are, respectively, the spin (orbital) moment, total (core), and s-electron (non-s-electron) hyperfine fields. Cu(Au)n denotes Cu(Au) in the nth layer below the interface Cu(Au) layer.

System	Atom	m_s	m_o	$B_{\rm hf}$	$B^c_{\rm hf}$	$B^s_{\rm hf}$	$B^{\rm ns}_{\rm hf}$
Fe_2Cu_6 fcc (001)	Cu	0.069	0.005	−120.4	−12.4	−113.7	5.6
	Cu1	−0.006	0.0	−22.3	0.1	−22.4	0.1
	Cu2	0.003	0.0	4.1	−0.2	4.2	0.1
Fe_2Cu_6 fcc (001)[a]	Cu	0.069	0.005	−120.0	−12.4	−113.5	5.7
	Cu1	−0.006	0.0	−22.3	0.1	−22.3	−0.1
	Cu2	0.003	0.0	4.9	−0.2	4.5	0.5
Fe_1Cu_5 fcc (001)	Cu	0.035	0.005	−115.9	−9.8	−110.8	4.7
	Cu1	−0.015	−0.001	−20.7	0.6	−29.4	8.1
	Cu2	0.001	0.0	5.4	−0.1	5.4	0.1
Fe_1Cu_5 fcc (001)[a]	Cu	0.035	0.004	−115.4	−9.8	−110.8	5.2
	Cu1	0.015	0.0	−20.5	0.6	−29.4	8.4
	Cu2	0.001	−0.001	5.1	−0.1	5.7	−0.5
bcc Fe_1/fcc Au_5 (001)	Au	0.031	0.021	−1062.4	−63.1	−1015.7	16.4
	Au1	−0.014	−0.004	−284.1	1.8	−284.7	0.8
	Au2	0.0	0.002	−107.1	−1.9	−119.1	13.9
bcc Fe_1/fcc Au_5 (001)[a]	Au	0.031	0.027	−992.9	−63.1	−1016.2	86.3
	Au1	−0.015	−0.004	−284.1	1.8	−286.7	0.9
	Au2	0.0	0.0	−124.8	−1.9	−116.3	6.6
bcc Fe_3/fcc Au_5 (001)	Au	0.061	0.021	−876.0	−70.7	−822.5	17.2
	Au1	−0.008	−0.003	195.4	−0.1	52.3	143.2
	Au2	−0.004	0.002	−75.1	0.4	−87.0	11.0
bcc Fe_3/fcc Au_5 (001)[a]	Au	0.061	0.028	−811.2	−70.7	−819.0	78.5
	Au1	−0.009	−0.002	196.1	−0.1	51.2	145.0
	Au2	−0.003	0.0	−85.7	0.4	−82.9	−3.1
bcc Fe_7/fcc Au_5 (001)	Au	0.068	0.022	−915.3	−74.7	−855.5	14.9
	Au1	−0.005	−0.002	169.9	−1.6	40.7	130.9
	Au2	−0.001	0.002	−68.8	0.1	−83.0	14.1
bcc Fe_7/fcc Au_5 (001)[a]	Au	0.067	0.029	−889.8	−74.7	815.1	46.2
	Au1	−0.004	−0.001	169.9	−1.6	39.2	132.1
	Au2	−0.001	0.001	−82.1	0.1	−79.1	−3.1

[a]In-plane magnetization.

B. Co multilayers

Calculated magnetic moments and hyperfine fields of Co in the Co multilayers are presented in Table VI. The orbital hyperfine field ($B^o_{\rm hf}$) is derived from the calculated non-s-electron hyperfine field ($B^{\rm ns}_{\rm hf}$), orbital moment (m_o), and magnetic dipole moment (m_d) by using Eqs. (7c). As in the Fe multilayers, the Co hyperfine field in the interface Co monolayers is considerably reduced compared with that in the bulk Co and also in the interior Co monolayers (Table IV). Unlike in the Fe multilayers, the s-electron hyperfine field in the interface Co monolayers is substantially reduced but does not change sign in all the Co multilayers except $CoPd_5$ fcc (111). The non-s-electron hyperfine field is generally larger in the Co multilayers than in the Fe multilayers, and this can be correlated with the larger orbital moment in the former (see Tables IV and VI).

There is a pronounced hyperfine-field anisotropy in these Co multilayers too, but the anisotropy is generally smaller than in the Fe multilayers. Interestingly, in all the Fe and Co multilayers except Co_2Cu_6 fcc (001) studied in this work, the value of the (negative) hyperfine field in the interface Fe (Co) monolayers is larger for the in-plane magnetization than for the perpendicular magnetization (see Tables IV and VI). This can be correlated with the corresponding larger orbital moment and non-s-electron hyperfine field (positive value) for the perpendicular magnetization. With the change of the magnetization from the in-plane to the perpendicular orientation, the magnetic dipole moment generally changes sign from positive to negative in the Fe multilayers but from negative to positive in the Co multilayers. According to Eqs. (7a) and (7b), therefore, the magnetic dipole hyperfine-field anisotropy will generally enforce the orbital hyperfine field anisotropy in the Fe multilayers but reduce the orbital hyperfine field anisotropy in the Co multilayers. Finally, it is clear from Table VI that the variation of the nonmagnetic Pt slab thickness does not significantly change the Co hyperfine field in the interface Co monolayers when the Pt slabs are thicker than, say, four monolayers.

TABLE VI. Calculated magnetic moments (μ_B/atom) and hyperfine fields (kG) of Co in hcp Co and Co multilayers. m_s (m_o), $B_{\rm hf}$ ($B^c_{\rm hf}$), and $B^s_{\rm hf}$ ($B^{\rm ns}_{\rm hf}$) are, respectively, the spin (orbital) moment, total (core) and s-electron (non-s-electron) hyperfine fields. m_d and $B^o_{\rm hf}$ are, respectively, the magnetic dipole moment and the orbital hyperfine field. Co n denotes Co in the nth layer below the interface Co layer.

System	Atom	m_s	m_o	m_d	$B_{\rm hf}$	$B^c_{\rm hf}$	$B^s_{\rm hf}$	$B^{\rm ns}_{\rm hf}$	$B^o_{\rm hf}$
hcp Co		1.596	0.077	−0.006	−225.2	−190.5	−85.2	50.5	48.4
Co_2Cu_6	Co	1.548	0.086	−0.012	−157.8	−184.0	−19.4	55.6	50.3
Co_2Cu_6[a]		1.549	0.095	0.007	−152.7	−184.0	−19.4	60.7	62.9
Co_1Pd_5	Co	1.961	0.131	−0.049	−84.5	−219.1	28.8	105.8	89.1
Co_1Pd_5[a]		1.960	0.094	0.026	−143.0	−219.1	28.9	47.2	54.8
Co_2Pd_4	Co	1.854	0.132	0.029	−156.9	−218.5	−17.4	79.0	88.7
Co_2Pd_4[a]		1.853	0.100	−0.014	−169.7	−218.5	−17.2	61.1	57.2
Co_3Pd_3	Co	1.879	0.128	0.023	−163.2	−220.3	−22.0	79.0	86.7
	Co1	1.744	0.109	0.068	−202.0	−206.1	−47.7	50.9	74.0
Co_3Pd_3[a]	Co	1.879	0.104	−0.010	−174.3	−220.3	−21.9	67.9	64.7
	Co1	1.745	0.099	−0.034	−178.8	−206.1	−46.5	73.8	63.1
Co_2Pt_1	Co	1.853	0.119	0.032	−184.2	−215.1	−38.2	69.2	79.9
Co_2Pt_1[a]		1.854	0.081	−0.016	−200.6	−215.1	−37.5	52.2	47.6
Co_2Pt_4	Co	1.896	0.119	0.036	−163.9	−216.6	−15.4	68.1	80.2
Co_2Pt_4[a]		1.896	0.073	−0.017	−185.4	−216.6	−15.3	46.5	41.7
Co_2Pt_7	Co	1.907	0.120	0.035	−163.2	−216.9	−15.2	68.9	80.7
Co_2Pt_7[a]		1.907	0.075	−0.017	−184.3	−216.9	−15.1	47.7	42.8

[a]In-plane magnetization.

V. DISCUSSION

A. Relations between magnetic moments and hyperfine fields

As noted in Sec. III, the non-s-core electron contributions to the hyperfine field are tiny, and the core part of the hyperfine field is almost entirely due to the s-electron contribution (the Fermi contact term), which measure the induced core polarization in the vicinity of the nuclei by the valence electrons. Therefore, one may expect that the core hyperfine field ($B^c_{\rm hf}$) be proportional to the spin moment (m_s). The calculated core hyperfine field in the Fe and Co multilayers is plotted against the calculated spin moment in Fig. 1. Indeed, as found before (see, e.g., Refs. 14, 21–23, 25–26, and 42), the core hyperfine field $B^c_{\rm hf}$ of Fe (Co) follows closely the variation of the spin moment m_s (see Fig. 1). The linear constant (or the slope) ($R = B^c_{\rm hf}/m_s$) is estimated to be around -113 kG/μ_B for both elements. Nevertheless, Fig. 1 indicates that R should be slightly larger for Co than for Fe. This increase of R along the $3d$ transition-metal series can be expected, since the s-core states get closer to the nucleus with an increasing atomic number Z. Figure 1 also suggests that the core hyperfine field can be rather reliably estimated from the spin moment by using this linear relationship, or vice versa.

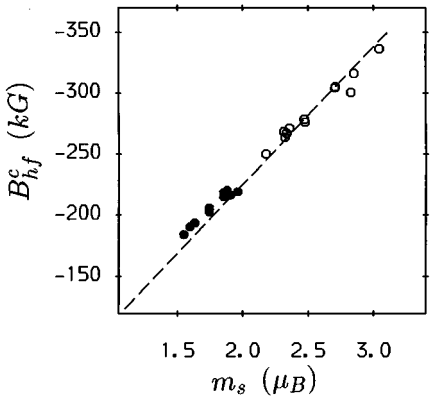

FIG. 1. The calculated core hyperfine field ($B^c_{\rm hf}$) vs the spin moment (m_s). The values are taken from Tables III, IV, and VI. Open circles denote the Fe atoms, and solid circles denote the Co atoms. The line is the guide to the eye only.

It has been found that in metals and alloys, the non-s hyperfine field, to some extent, is proportional to the orbital moment (see Refs. 25 and 26 and references therein). To see whether this also holds or not in the multilayers, we plot the non-s hyperfine field against the orbital moment in Fig. 2(a). Figure 2(a) indicates that although the points cluster along the straight lines, the deviations from the lines are large. Furthermore, most of the large deviations come from the points where the magnetic dipole moment is significant (bigger than 10% of the orbital moment) [denoted by squares in Fig. 2(a)]. This suggests that Eqs. (7b) may still hold in the multilayers if one subtracts the magnetic dipole hyperfine field from the non-s electron hyperfine field. The orbital hyperfine field, estimated by using Eqs. (7c) and data from Tables III, IV, and VI, is plotted in Fig. 2(b). It is clear from Fig. 2(b) that, to a rather good extent, the orbital hyperfine field is proportional to the orbital moment even in the multilayers. However, the linear coefficient (or the slope) $2\langle r^{-3}\rangle$ for Fe is different from that for Co. The expection value of r^{-3} ($\langle r^{-3}\rangle$) is estimated to be $3.38{a_0}^{-3}$ (a_0 is Bohr radius) for Fe and $4.97{a_0}^{-3}$ for Co. Note that $1\mu_B$ is equal to 6.264

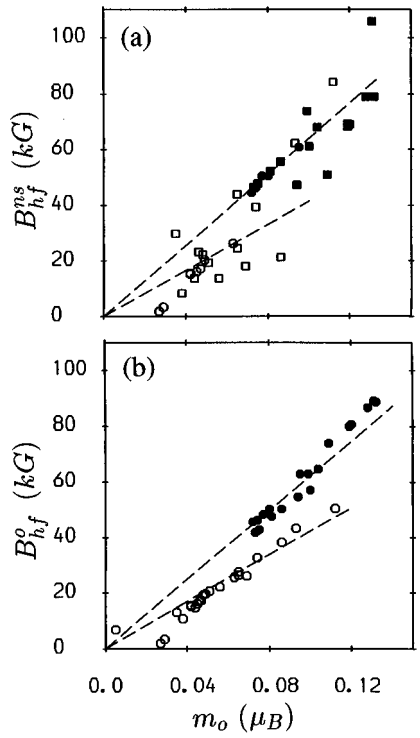

FIG. 2. (a) The calculated non-s-electron hyperfine field ($B^{\rm ns}_{\rm hf}$) vs the orbital moment (m_o) and (b) the estimated orbital hyperfine field ($B^{o}_{\rm hf}$) (see text) vs the orbital moment. The values are taken from Tables III, IV, and VI. Open circles and squares denote the Fe atoms. Solid circles and squares denote the Co atoms. Squares in (a) indicate the magnetic dipole moment (m_d) being greater than 10% of m_o and circles otherwise. The lines are merely the guide to the eye.

kG/$a_0{}^{-3}$. Obviously, $\langle r^{-3}\rangle$ for Co should be larger than that for Fe because of stronger localization of the Co wave function because of the bigger atomic number of Co. The calculated magnetic dipole field [$(B^{\rm ns}_{\rm hf}-B^{o}_{\rm hf})$ from Tables III, IV, and VI] is plotted against the magnetic dipole moment (m_d) in Fig. 3. It is clear that the magnetic dipole field is well proportional to the magnetic dipole moment. Furthermore, the straight lines in Fig. 3 were drawn by using the same value of $\langle r^{-3}\rangle$ as that of the corresponding lines in Fig. 2(b). In conclusion, the linear relations of Eqs. (7a) and (7b) hold rather well in magnetic multilayers.

However, there is no apparent correlation between the total hyperfine field ($B_{\rm hf}$) and the total magnetic moment Fe (Co) in the Fe (Co) multilayers (see Tables IV and VI). This is in contrast to the case of bulk metals and alloys where a rather close correlation between the variation of the measured hyperfine field with alloy composition and that of the averaged magnetic moment has been observed.[6] There is no obvious correlation between the total hyperfine field and the spin (or orbital or magnetic dipole) moment either. This is because of the complicated relationship between the s-electron valence hyperfine field and the spin (or total magnetic) moment. For the transition metals, the magnetic moments are dominated by the d-electron contributions. Unlike the core hyperfine field, which is determined only by the induced core polarization, the s-electron hyperfine field is

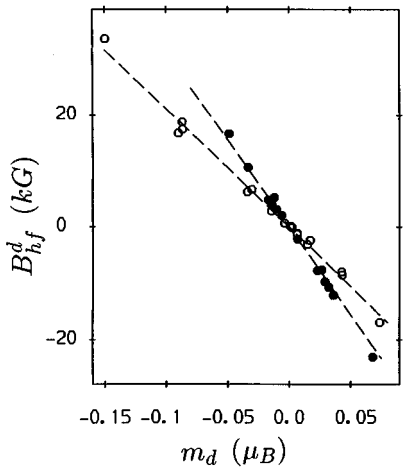

FIG. 3. The calculated magnetic dipole hyperfine field [$B^{d}_{\rm hf}$ or $(B^{\rm ns}_{\rm hf}-B^{o}_{\rm hf})$] (see text) vs the magnetic dipole moment (m_d). The values are taken from Tables III, IV, and VI. Open circles denote the Fe atoms and solid circles denote the Co atoms. The lines are drawn by using the same values of $\langle r^{-3}\rangle$ as those of the corresponding ones in Fig. 2(b) (see text).

determined by the balance of two competing effects, namely, the induced s-electron polarization by the d electrons and the direct s-electron polarization caused by the hybridization between the s and d orbitals.[22]

B. Comparison with experiment

Detailed comparison of the calculated hyperfine fields with experiment is difficult because the multilayers investigated in this work are highly idealized. Nevertheless, qualitative or semiquantitative comparison between experiment and theory can be made. For example, we also find an interface-induced Friedel oscillation in the hyperfine field in the Fe_7Au_5-fcc (001) multilayer, in qualitative agreement with experiments on the Fe(110) surface and W(100)/F(100) interface.[12,13] However, the observed reduction of the hyperfine field (about 20 kG) in the surface Fe monolayer[12] is only half of the predicted value of around 40 kG for in-plane magnetization (Table IV). Furthermore, this reduction was found to disappear upon coating the Fe(110) surface with silver.[12] Nevertheless, a large reduction of the interface Fe hyperfine field has been observed in the Fe/Cr multilayers, perhaps with sharper interfaces (108 kG) (Ref. 46) and at the W(100)/Fe(100) interface (about 200 kG) (Ref. 13). Recently, monolayer-probe ^{57}Fe Mössbauer effect measurements have been performed on the bcc-Fe/fcc-Ag (001) bilayers.[47] Several satellites were observed for the ^{57}Fe in the interface Fe monolayers, indicating the existence of the interface roughness. The field of the lowest satellite is -266 kG, which is considerably higher than -120–-170 kG found in the bcc-Fe_1/fcc-Ag_5 (001) superlattice but is close to -287 kG found in the bcc-Fe_7/fcc-Au_5 (001) with an in-plane magnetization (Table IV). The Au hyperfine fields in an Au(5 Å)/Fe(8 Å) superlattice have been measured.[4] Two observed components of -1050 and -570 kG can perhaps be assigned to the interface Au atoms and the interior Au atoms, respectively. The former is in reasonable agree-

ment with the present calculations for bcc-Fe_1/fcc-Au_5 (001), but the latter is twice as large as the corresponding calculated values (see Table V). The discrepancy may suggest that the latter Au atoms are partially exposed to the Fe atoms because of the interface imperfections in the superlattice.

No hyperfine-field measurement has been reported for the Co/Pt multilayers, to our knowledge, but ^{59}Co NMR experiments have been carried out for the Co/Pd multilayers.[48] However, the scanned field range from about -190 to -240 kG is believed to be too small to see the interface Co hyperfine fields. Several ^{59}Co NMR measurements have been carried out on the Co/Cu multilayers (see, e.g., Refs. 7 and 8), but only one report[8] on the Co_nCu_m fcc (001). Furthermore, four satellites were observed in the Co_nCu_m fcc (001),[8] and this was attributed to the interface roughness. Nevertheless, we note that the value of the third satellite (about -150 kG) is close to the theoretical Co hyperfine field (around -155 kG) in the Co_2Cu_6 fcc (001). The observed Co hyperfine field is usually interpreted in terms of the number (n^1) of the neighboring Co atoms (see, e.g., Refs. 7 and 8), i.e.,

$$B_{\rm hf} \approx B_{\rm hf}^b - \Delta B_{\rm hf}^1 (n^b - n^1), \tag{8}$$

where $B_{\rm hf}^b$ is the bulk hyperfine field, n^b is the Co coordination number in the corresponding bulk, and $\Delta B_{\rm hf}$ is about -18 kG.[7] Indeed, first-principles calculations by Ebert *et al.*[49] showed that at least in the Fe and Ni alloys, the hyperfine fields vary linearly with the number of Fe atoms within a given shell, and the changes because of simultaneous changes of the atomic configurations of different shells are additive. Nevertheless, Ebert *et al.*[49] also demonstrated that it is necessary to include a term due to the second-nearest neighbors in Eq. (8). We can use the results in Table VI to check Eq. (8) by taking $B_{\rm hf}^b$ as -222.8 kG (theoretical value for fcc Co). Simple arithmetic indicates that Eq. (8) works rather well for the perpendicular magnetization for all the Co systems studied except Co_1Pd_5 and Co_2Pt_1. This suggests that the large reduction in the Co hyperfine field in the interface monolayers is related to the corresponding reduction in the Co coordination number. However, Eq. (8) is less successful for the in-plane magnetization and, furthermore, the absolute value of $\Delta B_{\rm hf}$ has to be empirically increased by about 20 kG. This suggests that Eq. (8) should be used with caution, and perhaps the anisotropic hyperfine field should be taken into account. Finally, we note that Eq. (8) does not seem to hold for the Fe systems, possibly because the first-nearest-neighbor Fe (Co) bond length differs much more strongly in the different Fe systems than in the different Co systems. Of course, the variation of the first-nearest-neighbor bondlength is not taken into account in Eq. (8). However, it is not the purpose of this paper to present a detailed analysis on the validity of Eq. (8) and to design a more elaborate replacement of it.

C. Comments on previous and present calculations

There are several reports on previous hyperfine-field calculations for magnetic multilayers and thin films in the literature.[14,21–23,46] The results of these previous calculations are found to be in qualitative agreement with the present calculations. For example, they all found that the hyperfine field of Fe (or Co) in the surface or interface monolayers is substantially reduced. Freeman and co-workers predicted the surface-induced Friedel oscillation in the hyperfine field.[14] This was confirmed by subsequent experiments and calculations[12–13,46] and is also corroborated by the present results for bcc-Fe_7/fcc-Au_5 (001) (see Table IV). However, we notice that the theoretical hyperfine fields in both the bulks and multilayers reported by Freeman and co-workers (see Refs. 14, 21–23, and references therein) are systematically higher than those obtained in this work. For example, the hyperfine field for the bulk fcc Co is -306 kG from Ref. 23 compared with -222.8 kG from Table III. This pronounced discrepancy comes not only from the obvious fact that the non-*s*-electron contribution was neglected in these previous calculations but also from the outstanding differences in the core hyperfine field. The core hyperfine field to spin moment ratio obtained in Refs. 14 and 21–23 is around $-130 \sim -140$ kG/μ_B, being significantly larger than the value of about -110 kG/μ_B obtained in this work. As pointed out before,[50] in many all-electron electronic structure calculations of magnetic systems, including those of Freeman and co-workers,[14,21–23] the core electrons were treated ''relativistically'' by solving the Dirac equation twice, once for the majority spin potential and once for minority spin potential. This prescription, at most, amounts to an *ad hoc* relativistic treatment of the core electrons. The correct approach is to solve the spin-polarized Dirac equation,[17] as we have done in this work. It is believed that the discrepancy in the core hyperfine field is caused by this *ad hoc* relativistic treatment of the core electrons in the previous calculations.[14,21–23,43] Because of the smallness of the non-*s*-core electron contribution to the hyperfine field (see Ref. 17 and also Table I), correct scalar-relativistic treatment[20] already gives rise to a core hyperfine field that is close to that obtained by the fully relativistic treatment. It is demonstrated by the fact that the core hyperfine field to the spin moment ratio obtained by Blügel *et al.*[20] (about -110 kG/μ_B) is almost equal to that presented above.

So far we considered only the intra-atomic hyperfine field and have neglected the contributions from the spin moments on the other atoms in the same solid (i.e., inter-atomic hyperfine field) ($B_{\rm hf}^i$). According to Eq. (5), the interatomic field comes only from the magnetic dipole and orbital terms and, therefore, is small because of the factor r^{-3}. Furthermore, since the orbital moment is generally much smaller than the spin moment, the predominant contribution comes from the magnetic dipole term, which at an atomic site q, in the atomic sphere approximation and for a ferromagnet, is given by

$$B_{\rm hf}^i(q) \approx -\sum_{\mathbf{q}'\mathbf{R}} \frac{\mathbf{m}_{\mathbf{q}}}{|\mathbf{R}+\mathbf{q}-\mathbf{q}'|^3} \left\{ 1 - 3 \frac{[(\mathbf{R}+\mathbf{q}-\mathbf{q}')\cdot \widehat{\mathbf{m}_{\mathbf{q}}}]^2}{|\mathbf{R}+\mathbf{q}-\mathbf{q}'|^2} \right\}$$

$$= -\sum_{\mathbf{q}'} \mathbf{m}_{\mathbf{q}'} M_{qq'} \tag{9}$$

where $M_{qq'}$ is the so-called magnetic dipole Madelung constant between atoms q and q' in the unit cell[27] and $\mathbf{R}$ the lattice vector. For all the systems considered in this work, $FeAg_5$-fcc (001) is expected to have the largest interatomic hyperfine field because of its largest spin moment (see Tables IV and VI) and its smallest number (one) of magnetic mono-

layers in the magnetic slabs. Using the magnetic dipole Madelung constant given in Ref. 27 and the Fe spin moment in Table IV, we obtain an interatomic dipole field of 4.13 kG for in-plane magnetization and of -8.27 kG for perpendicular magnetization. These values are small compared with intra-atomic contributions to the hyperfine field. For cubic systems, the interatomic dipole field is zero and for hcp Co, it is less than 0.05 kG. Therefore, for simplicity, we have neglected the inter-atomic hyperfine field ($B_{\rm hf}^{i}$).

We note from Tables IV and VI that the calculated magnetic dipole moment (hyperfine field) for perpendicular magnetization is about twice that for in-plane magnetization but has an opposite sign. This is not surprising. In a nonrelativistic or scalar-relativistic theory, because of the axial symmetry of the multilayer systems, the magnetic dipole moments (hyperfine fields) for in-plane and perpendicular magnetizations obey the relation $m_d(B_{\rm hf}^{d}) = -2m_d^{*}(B_{\rm hf}^{d,*})$ ($*$ denotes the magnetic dipole moment (hyperfine field) for the in-plane magnetization). Deviations from this relation are caused by the distortions of the spin magnetization density due to the spin-orbit coupling. Thus, the small deviations of the Fe and Co magnetic dipole moments (hyperfine fields) from this relation found in the multilayers (Tables IV and VI) merely indicate that the spin-orbit coupling in the Fe and Co atoms is small. This is consistent with the small Fe and Co orbital magnetic moments found in the multilayer systems, which are also caused by the spin-orbit coupling.

Finally, we wish to point out that although the present local spin-density functional calculations produce spin moments and hyperfine fields for bulk Fe and Co that are generally in satisfactory agreement with experiments, the calculated orbital magnetic moments are usually too small by up to 50%.[51,52] According to Eq. (7b), the orbital hyperfine fields may also be underestimated. The consequence of this theoretical underestimation of the orbital hyperfine field may show up clearly in the calculated anisotropy in the hyperfine field, since the anisotropic orbital hyperfine field is important to the total anisotropic hyperfine field. Indeed, the calculated anisotropy in the hyperfine field in hcp Co (5.8 kG) is nearly 30% smaller than the experimental value (8 kG) (see Table II). This underestimation of the orbital magnetic moment and the orbital hyperfine field is caused by the assumption made in the relativistic spin density functional theory[15] that the effective magnetic field couples to the electron spin only. A pragmatic remedy is to include the so-called orbital-polarization correction term in an *ad hoc* manner.[52] Indeed, inclusion of the orbital-polarization correction usually bring the theoretical orbital magnetic moments in line with experiment.[51,52] It may be argued by using Eq. (7b) that any improved theories that correct the orbital moment would further increase the existing discrepancy of the hyperfine field in bcc Fe between theory and experiment (see Table I). Nevertheless, whether this would be the case remains to be seen, since these theories might change other contributions, such as the magnetic dipole term to the hyperfine field.

VI. CONCLUSIONS

We have performed all-electron self-consistent spin-polarized and relativistic electronic structure calculations for Fe and Co and their multilayers. We obtained the magnetic hyperfine fields as well as magnetic moments from these calculated electronic structures. The fully relativistic hyperfine interaction operator was used, and, therefore, both the orbital and magnetic dipole contributions to the hyperfine field, as well as the conventional Fermi contact term, were calculated. In the bulk Fe and Co, the calculated hyperfine field and its variation with both the crystalline structure and the magnetization orientation are in reasonable agreement with experiments. It was found that in order to obtain accurate hyperfine fields it is important to use an accurate parametrization of the local density exchange-correlation potential and a sufficiently large basis set to perform all-electron self-consistent calculations (see Sec. III), and to treat the core electrons relativistically in a correct manner.[20,17]

The hyperfine field of Fe (Co) in the interface monolayers in the magnetic multilayers is found to be substantially reduced compared with that in the corresponding bulk metal, in strong contrast to the highly enhanced magnetic moments in the same monolayers. Unlike in the bulk metals and alloys, the magnetic dipole moment in the multilayers has been predicted to be comparable to the orbital moment and, as a result, the magnetic dipole contribution to the hyperfine field is not negligible. It was demonstrated that the magnetic dipole and orbital contributions to the hyperfine field are nearly proportional to the magnetic dipole moment and the orbital moment, respectively. The anisotropy in the hyperfine field was found to be very pronounced and to be strongly connected with the large anisotropy in the orbital moment and magnetic dipole moment. It is hoped that these interesting results will encourage further experimental studies on the anisotropy in the hyperfine field in the multilayers, overlayers, and thin films with atomically sharp interfaces.

ACKNOWLEDGMENTS

This work benefits from a collaboration within the European Human Capital and Mobility Network *"Ab initio (from electronic structure) calculation of complex processes in materials"* (Contract No. ERBCHRXCT930369), and from the Relativistic Effects in Heavy Elements Programme of the European Science Foundation and the DFG Relativistic Programme.

[1] See, e.g., C. E. Johnson, Hyperfine Interact. **90**, 24 (1994), and references therein.

[2] E. L. Hahn, Phys. Rev. **80**, 580 (1950).

[3] Q. Y. Jin, Y. B. Xu, H. R. Zhai, C. Hu, M. Lu, Q. S. Bie, Y. Zhai, G. L. Dunifer, R. Naik, and M. Ahmad, Phys. Rev. Lett. **72**, 768 (1994).

[4] Y. Kobayashi, S. Nasu, T. Emoto, and T. Shinjo, Hyperfine Interact. **94**, 2273 (1994).

[5] M. Kawakami, H. Enokiya, and T. Okamoto, J. Phys. F **15**, 1613 (1985).

[6] C. E. Johnson, M. S. Ridout, and T. E. Cranshaw, Proc. Phys. Soc. **81**, 1079 (1963).

[7] H. A. M. de Gronckel, K. Kopinga, W. J. M. de Jonge, P. Panissod, J. P. Schillé, and F. J. A. der Broeder, Phys. Rev. B **44**, 9100 (1991).
[8] Y. Suzuki, T. Katayama, and H. Yasuoka, J. Magn. Magn. Mater. **104-107**, 1843 (1992).
[9] G. Bayreuther, Hyperfine Interact. **47**, 237 (1989).
[10] N. C. Koon, B. T. Jonker, F. A. Volkening, J. J. Krebs, and G. A. Prinz, Phys. Rev. Lett. **59**, 2463 (1987).
[11] O. F. Bakkaloglu, M. F. Thomas, R. J. Pollard, P. J. Grundy, V. Lewis, and K. O'Grady, J. Magn. Magn. Mater. **125**, 209 (1993).
[12] J. Korecki and U. Gradmann, Europhys. Lett. **2**, 651 (1986).
[13] G. Liu and U. Gradmann, J. Magn. Magn. Mater. **118**, 99 (1993).
[14] S. Ohnishi, M. Weinert, and A. J. Freeman, Phys. Rev. B **30**, 36 (1984).
[15] A. H. MacDonald and S. H. Vosko, J. Phys. C **17**, 3355 (1979).
[16] H. Ebert, Phys. Rev. B **38**, 9391 (1988).
[17] H. Ebert, J. Phys.: Condens. Matter **1**, 9111 (1989).
[18] G. Breit, Phys. Rev. **35**, 1447 (1930).
[19] L. Tterlikis, S. D. Mahanti, and T. P. Das, Phys. Rev. **176**, 10 (1968).
[20] S. Blügel, H. Akai, R. Zeller, and P. H. Dederichs, Phys. Rev. B **35**, 3271 (1987).
[21] C. L. Fu and A. J. Freeman, Phys. Rev. B **35**, 925 (1987).
[22] S. C. Hong, A. J. Freeman, and C. L. Fu, Phys. Rev. B **38**, 12 156 (1988).
[23] C. Li, A. J. Freeman, and C. L. Fu, J. Magn. Magn. Mater. **83**, 51 (1990).
[24] D. D. Koelling and B. N. Harmon, J. Phys. C **5**, 3109 (1977).
[25] H. Ebert, P. Strange, and B. L. Gyorffy, Hyperfine Interact. **51**, 929 (1989).
[26] H. Ebert and H. Akai, Hyperfine Interact. **78**, 361 (1993).
[27] G. Y. Guo, W. M. Temmerman, and H. Ebert, J. Phys.: Condens. Matter **3**, 8205 (1991).
[28] G. Y. Guo and H. Ebert, Phys. Rev. B **50**, 10 377 (1994).
[29] M. E. Rose, *Relativistic Electron Theory* (Wiley, New York, 1961).
[30] W. M. Temmerman, P. A. Sterne, G. Y. Guo, and Z. Szotek, Molecular Simulation **4**, 153 (1989).
[31] O. Jepsen and O. K. Andersen, Solid State Commun. **9**, 1763 (1971).
[32] R. Wu and A. J. Freeman, Phys. Rev. Lett. **73**, 1994 (1994).
[33] G. Y. Guo, H. Ebert, W. M. Temmerman, and P. J. Durham, J. Magn. Magn. Mater. **148**, 66 (1995).
[34] P. Carra, B. T. Thole, M. Altarelli, and X.-D. Wang, Phys. Rev. Lett. **70**, 694 (1993).
[35] A. Abragam and M. H. L. Pryce, Proc. R. Soc. London, Ser. A **205**, 135 (1951).
[36] P. C. Riedi, T. Dumelow, M. Rubinstein, G. A. Prinz, and S. B. Qadri, Phys. Rev. B **36**, 4595 (1987).
[37] S. H. Vosko, L. Wilk, and M. Nusair, Can. J. Phys. **58**, 1200 (1980).
[38] G. Y. Guo and H. Ebert, Phys. Rev. B **51**, 12 633 (1995).
[39] U. von Barth and L. Hedin, J. Phys. C **5**, 1629 (1972).
[40] M. Kawakami, T. Hihara, Y. Koi, and T. Wakiyama, J. Phys. Soc. Jpn. **33**, 159 (1972).
[41] P. C. Riedi, Phys. Rev. B **8**, 5243 (1973).
[42] J. F. Janak, Phys. Rev. B **20**, 2206 (1979).
[43] B. Lindgren and J. Sjöström, J. Phys. F **18**, 1563 (1988).
[44] G. A. Prinz, Phys. Rev. Lett. **54**, 1051 (1985).
[45] P. M. Marcus and V. L. Moruzzi, Solid State Commun. **55**, 971 (1985).
[46] Ch. Sauer, J. Landes, W. Zinn, and H. Ebert, in *Magnetic Thin Films, Multilayers, and Surfaces*, edited by S. S. P. Parkin, MRS Symposia Proceedings No. 231 (Materials Research Society, Pittsburgh, 1992), p. 153.
[47] P. J. Schurer, Z. Celinski, and B. Heinrich, Phys. Rev. B **51**, 2506 (1995).
[48] H. A. M. de Gronckel, J. A. W. Derkx, K. Kopinga, and W. J. M. de Jonge, Hyperfine Interact. **51**, 1095 (1989).
[49] H. Ebert, H. Winter, B. L. Gyorffy, D. D. Johnson, and F. J. Pinski, Solid State Commun. **64**, 1011 (1987).
[50] G. Y. Guo, H. Ebert, W. M. Temmerman, K. Schwarz, and P. Blaha, Solid State Commun. **79**, 121 (1991).
[51] D. Weller, Y. Wu, J. Stöhr, and M. G. Samant, Phys. Rev. B **49**, 12 888 (1994).
[52] M. S. S. Brooks, Physica B **130**, 6 (1985); O. Eriksson, M. S. S. Brooks, and B. Johansson, Phys. Rev. B **41**, 9087 (1990); M. R. Norman, Phys. Rev. Lett. **64**, 1162 (1990).